

# Whole exome sequencing identified a homozygous novel mutation in *SUOX* gene causes extremely rare autosomal recessive isolated sulfite oxidase deficiency and literature review

**Rui Zhang**

Shenzhen Bao An Peoples Hospital

**Yajing Hao**

Shenzhen Bao An Peoples Hospital

**Ying Xu**

Shenzhen Bao An Peoples Hospital

**Jiale Qin**

Zhejiang University School of Medicine

**Yanfang Wang**

Shenzhen Bao An Peoples Hospital

**Subrata Kumar Dey**

West Bengal University of Technology: Maulana Abul Kalam Azad University of Technology

**Chen Li**

Zhejiang University School of Medicine

**Huilin Wang**

Shenzhen Bao An Peoples Hospital

**Santasree Banerjee** (✉ [santasree.banerjee@yahoo.com](mailto:santasree.banerjee@yahoo.com))

Jilin University <https://orcid.org/0000-0003-2481-4562>

---

## Primary research

**Keywords:** ISOD syndrome, SUOX gene, novel variant, homozygous, loss-of-function mutation

**Posted Date:** October 12th, 2021

**DOI:** <https://doi.org/10.21203/rs.3.rs-74199/v3>

**License:**  This work is licensed under a Creative Commons Attribution 4.0 International License. [Read Full License](#)

---

## Abstract

**Background:** Isolated sulfite oxidase deficiency (ISOD) is the rarest types of life-threatening neurometabolic disorders characterized by neonatal intractable seizures and severe developmental delay with an autosomal recessive mode of inheritance. ISOD is extremely rare and till date only 32 mutations have been identified and reported worldwide. Germline mutation in *SUOX* gene causes ISOD.

**Methods:** Here, we investigated a 5-days old Chinese female child, presented with intermittent tremor or seizures of limbs, neonatal encephalopathy, subarachnoid cyst and haemorrhage, dysplasia of corpus callosum, neonatal convulsion, respiratory failure, cardiac failure, hyperlactatemia, severe metabolic acidosis, hyperglycemia, hyperkalemia, moderate anemia, atrioventricular block and complete right bundle branch block.

**Results:** Whole exome sequencing identified a novel homozygous transition (c.1227G>A) in exon 6 of the *SUOX* gene in the proband. This novel homozygous variant leads to the formation of a truncated sulfite oxidase (p.Trp409\*) of 408 amino acids. Hence, it is a *loss-of-function* variant. Proband's father and mother is carrying this novel variant in a heterozygous state. This variant was not identified in 200 ethnically matched normal healthy control individuals.

**Conclusions:** Our study not only expand the mutational spectrum of *SUOX* gene associated ISOD, but also strongly suggested the application of whole exome sequencing for identifying candidate genes and novel disease-causing mutations.

## Background

Isolated sulfite oxidase deficiency (ISOD) [MIM# 272300] is one of the rarest types of neurometabolic disorders usually manifested with severe neurometabolic impairment and developmental delay.<sup>1,2</sup> ISOD patients with neonatal age of onset were usually characterized by very severe clinical phenotype which often leads to their death at their infancy.<sup>3</sup> Patients with ISOD were mostly presented with neonatal seizures, difficulties in feeding, high-pitched crying with irritation, severe developmental delay, abnormalities in muscle tone and movements.<sup>3</sup> Choreoathetosis and dystonia were very common in patients with ISOD.<sup>4</sup> In later stages, ectopia lentis was also identified in ISOD patients.<sup>3,5</sup> ISOD patients were also manifested with biochemical abnormalities, often included excess secretion of sulfites and S-sulfocysteine through urine and low level of cysteine in plasma.<sup>4</sup> In addition, neuroimaging of the ISOD patients usually showed diffuse cortical swelling which gradually and progressively leads to the multicystic encephalomalacia, mimicking hypoxic-ischemic encephalopathy.<sup>4,6</sup> In patients with ISOD, soon after birth, neuroimaging usually found hypoplastic corpus callosum and cerebral infraction, cystic supratentorial white matter degeneration, with signal intensity changes in bilateral basal ganglia and thalami.<sup>7,8</sup> ISOD patients with neonatal disease onset were often died soon after birth or during infancy.<sup>3</sup> However, ISOD patients, those who are not died at their neonatal stage, usually manifested with cerebral palsy, severe developmental delay and encephalomalacia later.

During literature review, we found that 27 reports of *SUOX* gene associated ISOD has been published till date.<sup>4-6,9-30</sup> Recently, five early-onset ISOD patients have been reported in Chinese population<sup>4,6,21,24,29</sup>, two early-onset patient in Chinese mainland<sup>27,28</sup>, and one late-onset ISOD pedigree including three patients have been reported in Chinese mainland<sup>30</sup>.

Germline mutation in *SUOX* gene causes Isolated sulfite oxidase deficiency (ISOD). *SUOX* gene is located at the long arm of the chromosome 12 (12q13.2) and encodes sulfite oxidase (SO) consisting of 545 amino acids.<sup>31</sup> Sulfite oxidase is located in the intermembrane space of mitochondria. Structurally, sulfite oxidase is consisting of two identical subunits (homodimer) and each subunit comprises of a N-terminal heme co-factor binding domain and a C-terminal molybdopterin-binding domain.<sup>32</sup> Firstly, for obtaining catalytic enzymatic activity, sulfite oxidase interacts and bind with a molybdenum-containing cofactor. Then, it catalyzes the transformation of sulfite (SO<sub>3</sub><sup>2-</sup>) to sulphate (SO<sub>4</sub><sup>2-</sup>) by oxidation via cytochrome c through which the oxidative degradation of the sulfur-containing amino acids (cysteine and methionine) has been taken place.<sup>33</sup> Germline mutations in *SUOX* gene leads to the formation of partial or complete non-functional sulfite oxidase, followed by the

impairment of the oxidative degradation of sulfite ( $\text{SO}_3^{2-}$ ) to sulfate ( $\text{SO}_4^{2-}$ ).<sup>20</sup> Partial or complete deficiency of sulfite oxidase leads to fatal neurological abnormalities at neonatal stage.

The patients with ISOD usually manifested with either fatal early-onset form presented with seizures, severe psychomotor retardation and death or late-onset form with comparatively milder clinical symptoms.<sup>9,19</sup> Genotype-phenotype relationship is quite clear, as type of mutation and residual sulfite oxidase activity is directly correlated with the disease severity.<sup>34</sup> Patients with ISOD clinically diagnosed by neuroimaging which identified multicystic leukoencephalopathy and atrophy of brain.<sup>14,20</sup> ISOD patient's laboratory test was majorly identified with positive urinary sulfite test, i.e. (i) increased level of S-sulfocysteine, taurine, and thiosulfate with normal level of uric acid in urine, (ii) high level of S-sulfocysteine and taurine, normal level of uric acid and methionine and low level of cystine and homocysteine in plasma.<sup>9</sup> Patients with ISOD harbouring homozygous or compound heterozygous mutation in *SUOX* gene were identified with complete loss of sulfite oxidase activity while asymptomatic carrier individual with heterozygous mutations in *SUOX* gene were usually presented with 50% loss of sulfite oxidase activity.<sup>14,35</sup>

In this study, we investigated a 5-days old Chinese female child with ISOD. Whole exome sequencing (WES) identified a novel homozygous transition (c.1227G>A) in exon 6 of the *SUOX* gene in the proband. This novel homozygous variant leads to the formation of a truncated sulfite oxidase (p.Trp409\*) of 408 amino acids. Hence, it is a *loss-of-function* variant. Proband's father and mother was harboring this novel variant in a heterozygous state. This variant leads to complete loss of *SUOX* mRNA and sulfite oxidase in the proband.

## Materials And Methods

### 2.1 Patients and Clinical Materials

In this study, a 5-days old Han Chinese female child with ISOD was recruited and enrolled in the Division of Maternal-Fetal Medicine, Bao'an Women and Children's Hospital, Jinan University, Shenzhen, China (Figure 1).

### 2.2 Radiological, Physical and Biochemical Examination

Ultrasonography (USG), magnetic resonance imaging (MRI) and computerized tomography (CT) were performed. Physical, biochemical and routine blood tests were performed in the proband. The proband was also tested for genetic metabolic diseases. Analysis of heme, reticulocyte and hsCRP has been done for the proband. Liver function, renal function, electrolyte and blood ammonia test were also undertaken for the proband. We also performed TroPI, myocardial enzyme and AMON test for the proband.

### 2.3 Whole exome sequencing (WES) and identification of candidate variants

Whole exome sequencing (WES) was performed for the proband. Genomic DNA of the proband was extracted from her peripheral blood according to the manufacturer's instructions. Genomic DNA of the proband was then subjected to WES. Sequences were captured by Agilent SureSelect version 6 (Agilent Technologies, Santa Clara, CA). Then, the enriched library was subjected to sequence with Illumina HighSeq 4000 platform. After that, the sequencing reads were aligned with GRCh37.p10 by using Burrows-Wheeler Aligner software (version 0.59). Next, Burrows-Wheeler aligned reads were locally aligned by using GATK Indel Realigner (broadinstitute.org/). Base quality recalibration of Burrows-Wheeler aligned reads was performed by the GATK Base Recalibrator (broadinstitute.org/). Then, we identified single-nucleotide variants (SNVs) and small insertions or deletions (InDels) by using GATK Unified Genotyper (broadinstitute.org/). Lastly, annotation of the identified variants with the Consensus Coding Sequences Database (20130630) at the National Center for Biotechnology Information (NCBI) was performed. The quality control data of WES has been illustrated in Table 1.

WES data were interpreted and analysed according to our previously published article.<sup>36,37</sup> Firstly, variants were selected based on their minor allele frequencies <0.01 in various databases (dbSNP, HapMap, 1000 Genomes Project and our database with

~50,000 Chinese Han samples). Secondly, identified variants were functionally classified into pathogenic, likely pathogenic, VUS, likely benign and benign groups according to the variant interpretation guidelines of American College of Medical Genetics and Genomics (ACMG).<sup>38</sup> Finally, the remaining variations in the proband and her unaffected were also analysed on the basis of the reference of the OMIM (<https://www.omim.org>) and other published resources.

## 2.4 Sanger sequencing

Sanger sequencing was performed for the proband as well as for his parents to validate the identified variants in WES. Primer pairs were designed for the candidate loci on the basis of reference genomic sequences of the Human Genome from GenBank in NCBI. Primers were synthesized (Invitrogen, Shanghai, China) and polymerase chain reaction (PCR) has been done by using an ABI 9700 Thermal Cycler. Then, PCR products were directly sequenced by an ABI PRISM 3730 automated sequencer (Applied Biosystems, Foster City, CA, USA). Sequencing data analysis was performed by DNASTAR SeqMan (DNASTAR, Madison, Wisconsin, USA).

Sanger sequencing validated the identified heterozygous variants by WES by using the following primers: F1 5'-GGCGGGCTATCACGTACGGG-3', R1 5'-GCGGCGTTCTATCGCCTATGCGG-3'. The reference sequence NM\_000456 of *SUOX* gene was used.

## 2.5 *In silico* Analysis

*In silico* analysis of identified variants was performed by Mutation Taster (<http://mutationtaster.org/>).<sup>39</sup>

# Results

## 3.1 Index case

In this study, we investigated a proband with ISOD from a nonconsanguineous Han Chinese family (Figure 1). Proband's elder sister was died and her parents were also phenotypically normal and asymptomatic.

In 2009, after a successful and uneventful pregnancy, proband's mother (I-2) gave birth to a baby girl (II-1). One hour after birth, she was identified with "general cyanosis" and consecutively transferred to the department of neonatology and pediatrics of our hospital for treatment. After admission, we found that the baby was unable for sucking milk and high tension of her quadrilateral muscles with spasmodic twitch. Then, we performed CT and found subarachnoid haemorrhage. Hence, we clinically diagnosed the baby girl with "neonatal hypoxic-ischemic encephalopathy with subarachnoid hemorrhage". The child died on the same day.

In 2019, proband's mother (I-2) achieved her second pregnancy. Prenatal examination identified no abnormalities. At 31 weeks of gestation, B-ultrasound was performed and found no abnormalities. However, at 37+4 weeks of gestation, B-ultrasound was performed again and showed that the left lateral ventricle was 1.12 cm wide (Figure 2.A), the depth of cisterna magna was 1.44 cm (Figure 2.B), there was a cystic area about 1.61cm × 0.91cm in size located in the midline of the brain above the anterior thalamus (Figure 2.C), and thin corpus callosum (Figure 2.D). At 38 weeks of gestation, MRI was performed and found that the posterior horn of bilateral ventricles was slightly widened, the third ventricles were enlarged and uplifted, connected with the longitudinal fissure cistern of the brain, and the possible absence of the corpus callosum was considered. There were many small and flaky abnormal signal shadows were identified in the white matter of bilateral frontotemporal lobe and bilateral basal ganglia, as well as many softened foci were found (Figure 2.E-H).

At 38+4 weeks of gestation, a live baby girl, the proband was born through a cesarean section. The birth weight of the proband was 3.17 kg, and the Apgar score was 10. Soon after delivery, the proband was identified with intermittent tremor or seizures in limb. Five days after birth, we also found that the proband was presented with intermittent tremor or seizures in limb, neonatal encephalopathy, subarachnoid haemorrhage, subarachnoid cyst, dysplasia of corpus callosum, neonatal convulsion,

hypotension, respiratory failure, heart failure, patent foramen ovale, hyperlactatemia, severe metabolic acidosis, hyperglycemia, hyperkalemia, moderate anemia, high atrioventricular block and complete right bundle branch block.

Combined with the prenatal MRI result and based on the clinical symptoms, the proband was immediately transferred to the neonatological department of our hospital. Emergency CT scan was performed and showed multiple hypodense lesions in bilateral, frontal and parietal cortex, symmetrical hyperdense shadows were identified in bilateral basal ganglia, dysplasia of corpus callosum, a small amount of subarachnoid hemorrhage, enlargement of cisterna magna, possible subarachnoid abscess and compression of cerebellar hemisphere (Figure 2. I-M).

After admission, the patient still had intermittent scream, obvious tremor or seizures in limb, decrease in oxygen saturation in blood and blood pressure under the sedative state with chloral hydrate. The proband was also sedated by the treatment with phenobarbital sodium, and the convulsion still occasionally occurred. Dopamine and dobutamine were continuously pumped to maintain normal blood pressure, while continuous positive airway pressure ventilation was used to maintain the normal blood oxygen.

The proband was tested for genetic metabolic diseases and found no abnormalities (Table 2). The proband was identified with high level of mean corpuscular volume (MCV), mean corpuscular hemoglobin (MCH), neutrophilic granulocyte percentage (NEUT%), immature cell percentage (IG%), NRBC%, NEUT, MONO#, IG#, NRBC#, RDW-SD, RDW-CV and IRF as well as low level of hemoglobin concentration (HGB), lymphocytes percentage (LYMPH%) and LFR (Table 3). Liver function, renal function, electrolyte and blood ammonia test of the proband showed extremely high level of GGT, high level of Aspartic transaminase (AST), AST/ALT and low level of Total protein (TP) and Albumin (ALB) (Table 4). We also performed TroPI, myocardial enzyme and AMON test for the proband and found extremely high level of Creatine Kinase (CK), Creatine kinase MB isoenzyme (CK-MB), Troponin (TroPI) and Ammonia (AMON) (Table 5).

On the 6th day of hospitalization, the proband was identified with a sudden weak breath, the heart rate dropped to about 80 times/ minute, the heart sound was low and blunt, the blood oxygen saturation dropped to about 70%, the blood pressure was 47/12 mmHg. The patient was immediately intubated with mechanical ventilation, the resuscitation capsule was pressurized with oxygen, and no improvement was found after external chest compression, and finally the proband died.

### 3.2 WES and Sanger sequencing identified a novel variant in *SUOX* gene

WES was performed for the proband. WES identified a novel homozygous variant (c.1227G>A) in exon 6 of the *SUOX* gene in the proband (Figure 3). This novel homozygous variant leads to the formation of a truncated sulfite oxidase (p.Trp409\*) of 408 amino acids instead of the wild type sulfite oxidase of 545 amino acids. Hence, it is a *loss-of-function* variants. Proband's father and mother was carrying the variant in a heterozygous state (Figure 3). This variant was not identified in the 200 ethnically matched normal healthy control individuals. This novel variant also not present in the Human Gene Variant database (HGMD, [www.hgmd.cf.ac.uk/](http://www.hgmd.cf.ac.uk/)), Online Mendelian Inheritance in Man (MIM, (<https://www.omim.org>)). This variant was not found in our inhouse database, consisting of ~ 50,000 Chinese Han samples. We also did not find this variant in ExAC, gnomAD, dbSNP and 1000 Genome Database. In this study, we also described the importance of WES as a potential sequencing technology for identifying candidate variant in the *SUOX* associated ISOD patients.

### 3.3 *In silico* Analysis

This variant (c.1227G>A, p.Trp409\*) were predicted as "disease causing" by Mutation Taster (<http://mutationtaster.org/>).<sup>39</sup>

## Discussion

In this study, we investigated a 5-days old Chinese girl child who was presented with Classic ISOD. Karyotype and chromosomal microarray analysis identified no chromosomal abnormalities in the patient. WES identified a novel homozygous transition (c.1227G>A) in exon 6 of the *SUOX* gene in the proband. This novel homozygous variant leads to the formation of a truncated sulfite oxidase (p.Trp409\*) of 408 amino acids instead of the wild type sulfite oxidase of 545 amino acids. Hence, it

is a loss-of-function variants. The proband's father and mother is carrying the variant in a heterozygous state. According to the variant interpretation guidelines of American College of Medical Genetics and Genomics (ACMG), this variant is categorized as "likely pathogenic" variant.<sup>38</sup>

The incidence of *SUOX* gene associated ISOD is very rare in Chinese population and only seven reports have been published yet.<sup>6,21,24,27-30</sup> Chan et al., reported a girl child presented with generalised tonicclonic convulsions, followed by opisthotonic posturing, generalised spasms with hypertonia, subsequent regression in development, recurrent convulsions, severe developmental delay, and difficulty in feeding.<sup>29</sup> Genetic molecular analysis has not been done for the proband.

In 2002, Lee et al., reported a ten-month-old boy characterized by neonatal seizures with elevated level of both sulphite and S-sulphocysteine in the urine while the uric acid level was normal in the blood. The proband was identified with a nonsense (c.1029C>G, p.Tyr343\*) mutation and a missense (c.479G>A, p.Arg160Gln) mutation.<sup>6</sup>

In 2012, Huang et al., investigated two patients with ISOD in Taiwan.<sup>21</sup> The reported a female new born presented with high-pitched cry, tonic movements of four limbs, seizures without desaturation, decreased level of total homocysteine in plasma, diffuse cerebral atrophy and persistent edema in the left occipital, posterior temporal, and parietal lobes. The proband was identified with a homozygous substitution (c.1200C>G, p.Tyr400\*) in *SUOX* gene.<sup>21</sup>

In 2017, Lee et al., reported a female new born clinically diagnosed with ISOD from Taiwan. The proband was manifested with difficulty in feeding and prolonged feeding time with poor sucking power. The proband was also presented with seizures with bicycling of legs, alternating myoclonic seizures with rhythmic jerking over limbs, and high-pitched irritable cry. Proband's brain MRI showed ventricular dilatation, left frontal and temporal areas with cystic lesions, high T2 signal intensity of the bilateral cerebral cortex and globus pallidi. The proband was identified with normal level of bicarbonate, ammonia, plasma uric acid, amino acids, acylcarnitine, and urinary organic acids with absence of sufites in urine as well as a very low level of plasma cysteine. The proband was identified with a homozygous substitution (c.1200C>G, p.Tyr400\*) in *SUOX* gene.<sup>24</sup> Here, our patient was presented with intermittent tremor or seizures of limbs, neonatal encephalopathy, subarachnoid cyst and haemorrhage, dysplasia of corpus callosum, neonatal convulsion, respiratory failure, cardiac failure, hyperlactatemia, severe metabolic acidosis, hyperglycemia, hyperkalemia, moderate anemia, atrioventricular block and complete right bundle branch block.

In 2019, Tian et al., reported three siblings (two males and one female) characterized by abnormalities in the bilateral globus pallidus and substantia nigra with decreased level of plasma homocysteine. Genetic molecular studies identified two novel compound heterozygous (c.1096C>T, p.Arg366Cys and c.1376G>A, p.Arg459Gln) mutations in the *SUOX* gene.<sup>30</sup>

Recently, Du et al., two offspring identified with a heterozygous nonsense pathogenic variant (c.1200C>G, p.Y400\*) and a heterozygous duplication (c.1549\_1574dup, p.I525 Mfs\*102) in the *SUOX* gene in the proband.<sup>27</sup> Lastly, Zhao et al., reported a Chinese new born patient presented with homocysteine and uric acid in plasma, cysteine and total homocysteine in the blood and S-sulfocysteine was abnormally elevated in urine.<sup>28</sup> The proband was manifested with progressive encephalopathy, tonic seizures, abnormal muscle tone, difficulties in feeding, progressive neuropathological findings, intermittent convulsions and axial dystonia.<sup>28</sup> The proband was identified with heterozygous novel nonsense variant (c.475G>T, p.Glu159\*) and a heterozygous missense variant (c.1201A>G, p.Lys401Glu) in the *SUOX* gene in the proband.<sup>28</sup>

Generally, ISOD is manifested with axial and peripheral hypotonia with movement abnormality, seizures, spasticity, microcephaly, intellectual deficit, difficulties in feeding, severe psychomotor retardation and ectopia lentis or dislocation of lens with an early infantile or neonatal age of onset. Axial and peripheral hypertonia are the most common phenotype among ISOD patients. Pharmaco-resistant seizures with abnormalities in muscle tone and movements were usually identified in most of the ISOD patients. Gradual and progressive difficulties in feeding was also found in many ISOD patients. According to neuropathological symptoms, it is impossible to distinguish between ISOD patients and the patients with severe perinatal asphyxia.<sup>40,41</sup> Zaki et al., strongly recommended to include ISOD in the new-born differential clinical diagnosis with neonatal convulsion, seizures, abnormalities in movement and EEG test result.<sup>15</sup> Previous studies showed that typical

neuropathological (progressive changes in white matter, atrophy of cerebrum and cerebellum, cystic leukomalacia and ventriculomegaly) features of ISOD patients usually identified by neuroimaging (CT or MRI).<sup>42,43</sup>

Till date, no curative treatment has been developed for the patients with ISOD. In human, catabolism of cysteine is the major source of sulfite, so, late-onset ISOD patients with milder clinical symptoms usually recommended with low-methionine or low-cysteine diet.<sup>9,44,45</sup> Previous study reported that two late-onset ISOD patients with mild clinical phenotype has been treated with low-methionine and low-cysteine diet and showed gradual progress in psychomotor development without neurological deterioration.<sup>44</sup> However, ISOD patients with early or neonatal age of onset usually showed lethal outcome.<sup>14</sup>

Sulfite oxidase is a molybdenum dependent enzyme containing three domains (Figure 4). Pre-sulfite oxidase translocated from the cytosol to the outer mitochondrial membrane through the N-terminal ladder peptide which subsequently anchored on the inner mitochondrial membrane.<sup>46</sup> Inner membrane peptidase (IMP) cleaved the N-terminal ladder peptide and the C-terminal fragment of sulfite oxidase has been released into the intermembrane space (IMS). Sulfite oxidase catalytically activated after binding with heme and molybdenum cofactor followed by homodimerization.<sup>42,46</sup>

Till now, only 32 germline variants of *SUOX* have been identified to be associated with ISOD. Among 32 reported variants, 20 variants are missense, 4 variants are nonsense, 6 variants are deletion which result into frameshift and one duplication.<sup>4,9-20,27,28</sup> One deletion leads to loss of the wild type stop codon and followed by formation of a prolonged protein (Table 6).<sup>13</sup>

ISOD is a very rare and extremely heterogenous disorder in terms of both genotype and phenotype. However, due to extreme genotypic and phenotypic heterogeneity among patients with ISOD, identifying candidate gene and disease-causing mutation is a great challenge. Genetic screening of ISOD patients by performing next generation sequencing, either single gene sequencing or sequencing of a panel of genes are not always able to identify the candidate variants underlying the disease phenotype in ISOD patients. In order to overcome these disadvantages, whole exome sequencing, especially WES is the most significant and recent sequencing technologies for identifying the candidate gene and disease-causing variants in patients with ISOD. WES is the most sophisticated and advanced technique considering for identifying the candidate gene variants allowing clinicians for making timely and proper clinical diagnosis (Han et al., 2020; Dai et al., 2019; Ng et al., 2010; Zheng et al., 2018). In conclusion, our present study not only report the first variant of *SUOX* gene in a patient with ISOD in Chinese population, but also describe the importance and application of WES as a potential high throughput sequencing technology for molecular genetic analysis for the patients with ISOD.

In summary, here, we report a Chinese patient identified with extremely rare ISOD. Our present study expanded the mutation spectrum of *SUOX* gene associated with ISOD. Here, we also illustrated the significance of WES for identifying the candidate gene and disease-causing variants in patients with ISOD. This study also helped the clinicians for making proper clinical diagnosis of the ISOD patients with germline mutation in *SUOX* gene.

## Declarations

### ACKNOWLEDGEMENTS

We are thankful to the proband and all the family members for participating in our study.

### AUTHORS' CONTRIBUTION

Conceptualization: S.B., H.W. and R.Z. Data curation: R.Z., Y.H., Y.X. and J.Q. Formal analysis: Y.W., S.K.D., C.L. Investigation: S.B., H.W. and R.Z. Methodology: Y.W., S.K.D., Y.H., J.Q. and C.L. Project administration: S.B. and H.W. Resources: S.B. and H.W. Super vision: S.B. and H.W. Writing-original draft: S.B., H.W., R.Z., C.L. and S.K.D.

### FUNDING

We also thankful to the Guangdong Enterprise Key Laboratory of Human Disease Genomics (2011A060906007).

## AVAILABILITY OF DATA

Study data for the primary analyses presented in this manuscript are available upon reasonable request from the corresponding author.

## ETHICS APPROVAL

The ethics committee of the Bao'an Women and Children's Hospital, Jinan University, Shenzhen, China, approved the study, according to the recommendations of the Declaration of Helsinki. Written informed consent were obtained from all the participant of this study. The proband and his family members provided written informed consent for the publication of the patient's identifiable information.

## CONSENT FOR PUBLICATION

The patient's parents signed a consent regarding publication of the case study.

## CONFLICT OF INTEREST STATEMENT

There are no competing interests for any author.

## References

1. Schwarz G, Mendel RR, Ribbe MW. Molybdenum cofactors, enzymes and pathways. *Nature*. 2009; 460: 839-847.
2. Schwarz G. Molybdenum cofactor and human disease. *Curr Opin Chem Biol*. 2016; 31: 179-187.
3. Brown GK, Scholem RD, Croll HB, Wraith JE, McGill JJ. Sulfite oxidase deficiency: clinical, neuroradiologic, and biochemical features in two new patients. *Neurology*. 1989; 39: 252-257.
4. Chen LW, Tsai YS, Huang CC. Prenatal multicystic encephalopathy in isolated sulfite oxidase deficiency with a novel mutation. *Pediatr Neurol*. 2014; 51: 181-182.
5. Claerhout H, Witters P, Régál L, et al. Isolated sulfite oxidase deficiency. *J Inherit Metab Dis*. 2018; 41: 101-108.
6. Lee H F, Mak BS, Chi CS, Tsai CR, Chen CH, Shu SG. A novel mutation in neonatal isolated sulphite oxidase deficiency. *Neuropediatrics*. 2002; 33: 174-179.
7. Carmi-Nawi N, Malinger G, Mandel H, Ichida K, Lerman-Sagie T, Lev D. Prenatal brain disruption in molybdenum cofactor deficiency. *J Child Neurol*. 2011; 26: 460-464.
8. Sass JO, Nakanishi T, Sato T, Shimizu A. New approaches towards laboratory diagnosis of isolated sulphite oxidase deficiency. *Ann Clin Biochem*. 2004; 41: 157-159.
9. Rocha S, Ferreira AC, Dias AI, Vieira JP, Sequeira S. Sulfite oxidase deficiency-an unusual late and mild presentation. *Brain Dev*. 2014; 36: 176-179.
10. Bastarache L, Hughey JJ, Hebbring S, et al. Phenotype risk scores identify patients with unrecognized Mendelian disease patterns. *Science*. 2018; 359: 1233-1239.
11. Brumar D, Guerin E, Voegeli AC, Eyer D, Maitre M. A compound heterozygote case of isolated sulfite oxidase deficiency. *Mol Genet Metab Rep*. 2017; 12: 99-102.
12. Kisker C, Schindelin H, Pacheco A, et al. Molecular basis of sulfite oxidase deficiency from the structure of sulfite oxidase. *Cell*. 1997; 91: 973-983.
13. Johnson JL, Coyne KE, Garrett RM, et al. Isolated sulfite oxidase deficiency: identification of 12 novel SUOX mutations in 10 patients. *Hum Mutat*. 2002; 20: 74.
14. Johnson JL, Rajagopalan KV, Renier WO, Van der Burgt I, Ruitenbeek W. Isolated sulfite oxidase deficiency: mutation analysis and DNA-based prenatal diagnosis. *Prenat. Diagn*. 2002; 22: 433-436.



15. Zaki MS, Selim L, El-Bassyouni HT, et al. Molybdenum cofactor and isolated sulphite oxidase deficiencies: Clinical and molecular spectrum among Egyptian patients. *Eur J Paediatr Neurol.* 2016; 20: 714-722.
16. Bi C, Wu J, Jiang T, et al. Mutations of ANK3 identified by exome sequencing are associated with autism susceptibility. *Hum Mutat.* 2012; 33: 1635-1638.
17. Seidahmed MZ, Alyamani EA, Rashed MS, et al. Total truncation of the molybdopterin/dimerization domains of SUOX protein in an Arab family with isolated sulfite oxidase deficiency. *Am J Med Genet A.* 2005; 136: 205-209.
18. Rupar CA, Gillett J, Gordon BA, et al. Isolated sulfite oxidase deficiency. *Neuropediatrics.* 1996; 27: 299-304.
19. Salih MA, Bosley TM, Alorainy IA, et al. Preimplantation genetic diagnosis in isolated sulphite oxidase deficiency. *Can J Neurol Sci.* 2013; 40: 109-112.
20. Tan WH, Eichler FS, Hoda S, et al. Isolated sulfite oxidase deficiency: a case report with a novel mutation and review of the literature. *Pediatrics.* 2005; 116: 757-766.
21. Huang YL, Lin DS, Huang JK, Chiu NC, Ho CS. <sup>99m</sup>Tc-ethyl cysteinyl dimer cranial single-photon emission computed tomography and serial cranial magnetic resonance imaging in a girl with isolated sulfite oxidase deficiency. *Pediatr Neurol.* 2012; 47: 44-46.
22. van der Klei-van Moorsel JM, Smit LM, Brockstedt M, Jakobs C, Dorche C, Duran M. Infantile isolated sulphite oxidase deficiency: report of a case with negative sulphite test and normal sulphate excretion. *Eur J Pediatr.* 1991; 150: 196-197.
23. Garrett RM, Johnson JL, Graf TN, Feigenbaum A, Rajagopalan KV. Human sulfite oxidase R160Q: identification of the mutation in a sulfite oxidase-deficient patient and expression and characterization of the mutant enzyme. *Proc Natl Acad Sci USA.* 1998; 95: 6394-6398.
24. Lee HF, Chi CS, Tsai CR, Chen HC, Lee IC. Prenatal brain disruption in isolated sulfite oxidase deficiency. *Orphanet J Rare Dis.* 2017; 12: 115.
25. Mhanni AA, Greenberg CR, Spriggs EL, Agatep R, Sisk RR, Prasad C. Isolated sulfite oxidase deficiency: a founder mutation. *Cold Spring Harb Mol Case Stud.* 2020; 6: a005900.
26. Sharawat IK, Saini L, Singanamala B, et al. Metabolic crisis after trivial head trauma in late-onset isolated sulfite oxidase deficiency: Report of two new cases and review of published patients. *Brain Dev.* 2020; 42: 157-164.
27. Du P, Hassan RN, Luo H, et al. Identification of a novel SUOX pathogenic variants as the cause of isolated sulfite oxidase deficiency in a Chinese pedigree. *Mol Genet Genom Med.* 2021; 9: e1590.
28. Zhao J, An Y, Jiang H, Wu H, Che F, Yang Y. Novel Compound Heterozygous Pathogenic Variants in SUOX Cause Isolated Sulfite Oxidase Deficiency in a Chinese Han Family. *Front Genet.* 2021; 12: 607085.
29. Chan YK, Li CK, Lai CK, Ng SF, Chan AYW. Infantile isolated sulphite oxidase deficiency in a Chinese family: a rare neurodegenerative disorder. *Hong Kong Med. J.* 2002; 8: 279-282.
30. Tian M, Qu Y, Huang L, et al. Stable clinical course in three siblings with late-onset isolated sulfite oxidase deficiency: a case series and literature review. *BMC Pediatr.* 2019; 19: 510.
31. Feng C, Tollin G, Enemark JH. Sulfite oxidizing enzymes. *Biochim Biophys Acta.* 2007; 1774: 527-539.
32. Davis AC, Johnson-Winters K, Arnold AR, Tollina G, Enemark JH. Kinetic results for mutations of conserved residues H304 and R309 of human sulfite oxidase point to mechanistic complexities. *Metallomics.* 2014; 6: 1664-1670.
33. Johnson-Winters K, Tollin G, Enemark JH. Elucidating the catalytic mechanism of sulfite oxidizing enzymes using structural, spectroscopic, and kinetic analyses. *Biochemistry.* 2010; 49: 7242-7254.
34. Schwahn BC, Van Spronsen FJ, Belaidi AA, et al. Efficacy and safety of cyclic pyranopterin monophosphate substitution in severe molybdenum cofactor deficiency type a: a prospective cohort study. *Lancet.* 2015; 386: 1955-1963.
35. Holder JL Jr, Agadi S, Reese W, Rehder C, Quach MM. Infantile spasms and hyperekplexia associated with isolated sulfite oxidase deficiency. *JAMA Neurol.* 2014; 71: 782-784.
36. Zhang R, Chen S, Han P, et al. Whole exome sequencing identified a homozygous novel variant in CEP290 gene causes Meckel syndrome. *J Cell Mol Med.* 2020; 24: 1906-1916.

37. An J, Yang J, Wang Y, et al. Targeted Next Generation Sequencing Revealed a Novel Homozygous Loss-of-Function Mutation in ILDR1 Gene Causes Autosomal Recessive Nonsyndromic Sensorineural Hearing Loss in a Chinese Family. *Front Genet.* 2019; 10: 1.
38. Richards S, Aziz N, Bale S, et al. Standards and guidelines for the interpretation of sequence variants: a joint consensus recommendation of the American College of Medical Genetics and Genomics and the Association for Molecular Pathology. *Genet Med.* 2015; 17: 405-424.
39. Schwarz JM, Cooper DN, Schuelke M, Seelow D. MutationTaster2: mutation prediction for the deep-sequencing age. *Nat Methods.* 2014; 11: 361-362.
40. Hobson E, Thomas S, Crofton PM, Murray AD, Dean J, Lloyd D. Isolated sulphite oxidase deficiency mimics the features of hypoxic ischaemic encephalopathy. *Eur J Pediatr.* 2005; 164, 655-659.
41. Tyagarajan SK, Fritschy JM. Gephyrin: a master regulator of neuronal function? *Nat Rev Neurosci.* 2014; 15: 141-156.
42. Klein JM, Schwarz G. Cofactor-dependent maturation of mammalian sulfite oxidase links two mitochondrial import pathways. *J Cell Sci.* 2012; 125: 4876-4885.
43. Terao M, Romão MJ, Leimkühler S, et al. Structure and function of mammalian aldehyde oxidases. *Arch Toxicol.* 2016; 90: 753-780.
44. Touati G, Rusthoven E, Depondt E, et al. Dietary therapy in two patients with a mild form of sulphite oxidase deficiency. Evidence for clinical and biological improvement. *J Inherit Metab Dis.* 2000; 23: 45-53.
45. Del M, Burlina AP, Sass J, et al. Metabolic stroke in a late-onset form of isolated sulfite oxidase deficiency. *Mol Genet Metab.* 2013; 108: 263-266.
46. Hahn A, Engelhard C, Reschke S, Teutloff C, Bittl R, Leimkühler S, Risse T. Structural insights into the incorporation of the Mo cofactor into sulfite oxidase from site-directed spin labeling. *Angew Chemie.* 2015; 54: 11865-11869.
47. Han P, Wei G, Cai K, et al. Identification and functional characterization of mutations in LPL gene causing severe hypertriglyceridaemia and acute pancreatitis. *J Cell Mol Med.* 2020; 24, 1286-1299.
48. Ng SB, Buckingham KJ, Lee C, et al. Exome sequencing identifies the cause of a mendelian disorder. *Nat Genet.* 2010; 42, 30-35.
49. Dai Y, Liang S, Dong X, et al. Whole exome sequencing identified a novel DAG1 mutation in a patient with rare, mild and late age of onset muscular dystrophy-dystroglycanopathy. *J Cell Mol Med.* 2019; 23, 811-818.
50. Zheng Y, Xu J, Liang S, Lin D, Banerjee S. Whole Exome Sequencing Identified a Novel Heterozygous Mutation in HMBS Gene in a Chinese Patient with Acute Intermittent Porphyria with Rare Type of Mild Anemia. *Front. Genet.* 2018; 9: 129.

## Tables

**Table 1.** Quality control data of whole exome sequencing (WES).

	Sequencing Quality Control Data	Proband
Total	Raw Reads (All reads)	418838956
	QC Fail reads	0
	Raw Data (Mb)	20801.97
	Paired Reads	415957187
	Mapped Reads	413620698
	Fraction of Mapped Reads	99.59%
	Mapped Data (Mb)	20763.17
	Fraction of Mapped Data (Mb)	99.59%
	Properly paired	403841443
	Fraction of Properly paired	97.68%
	Read and mate paired	412565879
	Fraction of Read and mate paired	99.25%
	Singletons	1055532
	Read and mate map to different chromosome	7616614
	Read1	207428583
	Read2	207429847
	Read1(rmdup)	119237721
	Read2(rmdup)	119227631
	forward strand reads	206876641
	backward strand reads	206779598
	PCR duplicate reads	175685891
	Fraction of PCR duplicate reads	42.76%
	Map quality cutoff value	20
	Map Quality above cutoff reads	375981835
	Fraction of Map Q reads in all reads	90.56%
	Fraction of Map Q reads in mapped reads	90.95%
Target	Target Reads	232188768
	Fraction of Target Reads in all reads	55.89%
	Fraction of Target Reads in mapped reads	56.37%
	Target Data (Mb)	10643.73
	Target Data Rmdup (Mb)	5819.92
	Fraction of Target Data in all data	50.95%
	Fraction of Target Data in mapped data	50.92%
	Len of region	58672379

	Average depth	180.79
	Average depth (rmdup)	98.97
	Coverage (>0x)	99.89%
	Coverage (>=4x)	99.73%
	Coverage (>=10x)	99.83%
	Coverage (>=30x)	95.98%
	Coverage (>=100x)	68.79%
	Target Region Count	199794
	Region covered > 0x	199684
	Fraction Region covered > 0x	99.85%
	Fraction Region covered >= 4x	99.74%
	Fraction Region covered >= 10x	99.76%
	Fraction Region covered >= 30x	96.59%
	Fraction Region covered >= 100x	69.58%
Flank	Flank size	200
	Len of region (not include target region)	70686543
	Average depth	36.85
	Flank Reads	74996722
	Fraction of flank Reads in all reads	18.91%
	Fraction of flank Reads in mapped reads	18.92%
	Flank Data (Mb)	2568.55
	Fraction of flank Data in all data	12.95%
	Fraction of flank Data in mapped data	12.89%
	Coverage (>0x)	97.95%
	Coverage (>=4x)	87.62%
	Coverage (>=10x)	61.91%
	Coverage (>=30x)	37.68%
	Coverage (>=100x)	10.19%

**Table 2. Screening of the patient for genetic metabolic diseases.**

Number	Test name	Result	Reference Interval	Number	Test name	Result	Reference Interval
1	Alanine (ALA)	231.316	62.9-650	26	Phenylalanine (PHE)	41.414	21-120
2	Methionine (MET)	28.466	5-55	27	Arginine (ARG)	5.721	1.64-66.5
3	Glycine (GLY)	439.893	98-1200	28	Tyrosine (TYR)	69.727	25.8-320
4	Proline (PRO)	268.081	49.8-500	29	Homocysteine (HCY)	1.91	5-20
5	Ornithine (ORN)	175.813	42-400	30	Leucine (LEU+ILE)	183.634	70-330
6	Citrulline (CIT)	13.613	4-45	31	Free Carnitine(C0)	13.888	8-60
7	Acetyl-L-Carnitine(C2)	14.542	3.4-57	32	Propionyl carnitine(C3)	1.913	0.2-5
8	Malonyl carnitine(C3DC+C4OH)	0.075	0.02-0.3	33	Butylcarnitine (C4)	0.195	0.05-0.53
9	Methyl malonyl carnitine(C4DC+C5OH)	0.212	0.07-0.61	34	Isopentyl carnitine(C5)	0.176	0.04-0.45
10	Methyl croton acyl carnitine(C5:1)	0.013	<0.12	35	Glutaryl carnitine(C5DC+C6OH)	0.09	0.01-0.3
11	Acyl carnitine(C10:2)	0.01	<0.12	36	Hexyl carnitine(C6)	0.024	0.01-0.15
12	Adipic carnitine(C6DC)	0.018	0.01-0.25	37	Octyl carnitine(C8)	0.028	0.02-0.2
13	Octenyl carnitine(C8:1)	0.025	0.02-0.38	38	Acyl carnitine(C10)	0.027	0.01-0.3
14	Acyl carnitine(C10:1)	0.033	0.01-0.27	39	Dodecyl carnitine(C12)	0.023	0.02-0.34
15	Dodecyl carnitine(C12:1)	0.014	0.01-0.3	40	Tetradecanoyl carnitine(C14)	0.111	0.02-0.5
16	Dodecyl carnitine(C14:1)	0.049	0.01-0.3	41	Sondiene acyl carnitine(C14:2)	0.01	<0.15
17	Trihydroxytetradecanoyl carnitine(C14OH)	0.006	<0.04	42	Trihydroxyl octadecyl carnitine(C18OH)	0.005	<0.05
18	Hexadecyl carnitine(C16)	1.345	0.15-6.31	43	Hexadecyl carnitine(C16:1)	0.118	0.01-0.46
19	Trihydroxyhexadecyl carnitine (C16:1OH)	0.02	<0.1	44	Trihydroxyhexadecyl carnitine(C16OH)	0.011	<0.06
20	Octadecyl carnitine(C18)	0.516	0.1-1.85	45	Octadecyl carnitine(C18:1)	0.582	0.17-3
21	Eighteen - diene acyl carnitine(C18:2)	0.111	0.06-0.87	46	Trihydroxyl octadecyl carnitine (C18:1OH)	0.01	<0.05
22	PHE/TYR	0.594	0.1-1.5	47	ARG/ORN	0.033	0.01-0.5
23	CIT/ARG	2.379	0.2-12	48	ORN/CIT	12.915	2.5-35
24	MET/PHE	0.155	0.05-1.3	49	LEU+ILE/PHE	4.434	
25	TYR/PHE	1.684	0.8-7.5	50	CIT/PHE	0.329	0.15-1

**Table 2. Heme analysis, reticulocyte analysis and hsCRP of the patient.**

Test name	Result	Unit	Reference Interval	Test name	Result	Unit	Reference Interval
hsCRP	<0.5	mg/L	0-10	LYMPH#	2.28	*10 <sup>9</sup> /L	1.26-3.35
white blood cell count (WBC)	26.8	*10 <sup>9</sup> /L	8-30	MONO#	1.73↑	*10 <sup>9</sup> /L	0.25-0.84
red blood cell count (RBC)	4.13	*10 <sup>12</sup> /L	3.2-6.3	EO#	0.23	*10 <sup>9</sup> /L	0.01-0.4
hemoglobin concentration (HGB)	150↓	g/L	152-235	BASO#	0.06	*10 <sup>9</sup> /L	0.01-0.07
Platelet Count (PLT)	272	*10 <sup>9</sup> /L	125-350	IG#	2.76↑	*10 <sup>9</sup> /L	0-0.06
Hematokrit (HCT)	44.5	%	38-70	NRBC#	0.07↑	*10 <sup>9</sup> /L	0-0
mean corpuscular volume (MCV)	107.7↑	fL	82-100	RDW-SD	59.9↑	fL	38.2-49.2
Mean Corpuscular Hemoglobin (MCH)	36.3↑	pg	27-34	RDW-CV	15.1↑		12.1-14.3
Mean Corpuscular Hemoglobin Concentration (MCHC)	337	g/L	316-354	PCT	0.28	%	0.18-0.39
neutrophilic granulocyte percentage (NEUT%)	83.9↑	%	42.9-74.3	PDW	10.5		9.9-15.4
lymphocytes percentage (LYMPH%)	8.5↓	%	18.3-45.7	MPV	10.1	fL	9.1-11.9
MONO%	6.5	%	4.2-11.8	P-LCR	25.1		19.7-42.2
EO%	0.9	%	0.2-5.3	RET%	3.8	%	2-6
BASO%	0.2	%	0.1-1	RET#	155.3	*10 <sup>9</sup> /L	36.3-195.7
Immature cell percentage (IG%)	10.3↑	%	0-0.6	RET-He	34.6	pg	30.3-36
NRBC%	0.3↑	%	0-0	IRF	38.4↑	%	3.1-13.4
NEUT#	22.5↑	*10 <sup>9</sup> /L	2.1-8.89	LFR	61.6↓	%	89.9-98.4

**Table 4. Liver function, renal function, electrolyte and blood ammonia test of the patient.**

Test name	Result	Unit	Reference Interval	Test method
Total protein (TP)	59↓	g/L	63-82	dry chemistry method
Albumin (ALB)	34↓	g/L	35-50	dry chemistry method
GLB	25	g/L	20-40	calculation
A/G	1.4		1.2-2.4	calculation
TBIL	47.3	μmol/L	3-102.6	dry chemistry method
Bc	0	μmol/L	0-10	dry chemistry method
Bu	46.9	μmol/L	10-180	dry chemistry method
ALT	21	U/L	9-52	dry chemistry method
Aspartic transaminase (AST)	44↑	U/L	14-36	dry chemistry method
AST/ALT	2.1↑		0.8-1.5	calculation
GGT	405↑	U/L	12-43	dry chemistry method
ALP	223	U/L	0-500	dry chemistry method
Creatine	53	μmol/L	27-87	dry chemistry method
Urea	3.68	mmol/L	2.5-6.1	dry chemistry method
UA	340	μmol/L	149-446	dry chemistry method
K	3.94	mmol/L	3.5-5	dry chemistry method
Na	140	mmol/L	137-145	dry chemistry method

Table 5. TroPI, myocardial enzyme and AMON test of the patient.

Test name	Result	Unit	Reference Interval	Test method
Creatine Kinase (CK)	244↑	U/L	55-170	dry chemistry method
Creatine kinase MB isoenzyme (CK-MB)	10.9↑	ng/ml	0-2.37	chemiluminescence
LDH	464	U/L	313-618	dry chemistry method
Troponin (TroPI)	0.146↑	ng/ml	0-0.034	chemiluminescence
Ammonia (AMON)	133.6↑	μmol/L	9-33	dry chemistry method
LAC	>24 PH	mmol/L	0.7-2.1	dry chemistry method

Table 6: All reported variants in the *SUOX* gene (NM\_000456) associated with ISOD.

<b>Nucleotide changes</b>	<b>Amino acid change</b>	<b>Domain</b>	<b>Reference</b>
c.1227G>A	p.Trp409*	Homodimerization	Present Study
c.475G>T	p.Glu159*	Cyt-b5	Zhao et al., 2021
c.1201A>G	p.Lys401Glu	MoCo	Zhao et al., 2021
c.182T>C	p.Leu61Pro	Transit peptide	Rocha et al., 2014
c.287dupC	p.Glu97*	Cyt-b5	Johnson et al., 2002
c.352C>T	p.His118Tyr	Cyt-b5	Brumaru et al., 2017
c.427C>A	p.His143Asn	Cyt-b5	Del Rizzo et al., 2013
c.520delG	p.Asp174Thrfs*13	Hinge	Seidahmed et al., 2005
c.571_574delCAGC	p.Gln191Glyfs*12	MoCo domain	Johnson et al., 2002
c.571delC	p.Gln191Serfs*13	MoCo domain	Rupar et al., 1996
c.649C>G	p.Arg217Gly	Molybdopterin-binding	Brumaru et al., 2017
c.650G>A	p.Arg217Gln	Molybdopterin-binding	Kisker et al., 1997 Lee et al., 2002 Garrett et al., 1998
c.734_737delTTTC	p.Leu245Profs*27	MoCo domain	Johnson et al., 2002
c.772A>C	p.Ile258Leu	MoCo domain	Johnson et al., 2002
c.794C>A	p.Ala265Asp	MoCo domain	Kisker et al., 1997 Edwards et al., 1999
c.803G>A	p.Arg268Gln	MoCo domain	Johnson et al., 2002
c.884G>A	p.Gly295Glu	MoCo domain	Zaki et al., 2016
c.1084G>A	p.Gly362Ser	MoCo domain	Johnson et al., 2002
c.1096C>T	p.Arg366Cys	MoCo domain	Tian et al., 2019
c.1097G>A	p.Arg366His	MoCo domain	Johnson et al., 2002
c.1126C>T	p.Arg376Cys	MoCo domain	Johnson et al., 2002
c.1136A>G	p.Lys379Arg	Molybdopterin-binding	Johnson et al., 2002
c.1187A>G	p.Gln396Arg	MoCo domain	Johnson et al., 2002
c.1200C>G	p.Tyr400*	MoCo domain	Johnson et al., 2002
c.1234_1235delGT	p.Val412Argfs*3	Homodimerization	Salih et al., 2013
c.1261C>T	p.Gln421*	Homodimerization	Johnson et al., 2002
c.1280C>A	p.Ser427Tyr	Homodimerization	Edwards et al., 1999
c.1313_1316delTAGA	p.Val438Aspfs*5	Homodimerization	Tan et al., 2005
c.1348T>C	p.Trp450Arg	Homodimerization	Johnson et al., 2002
c.1355G>A	p.Gly452Asp	Homodimerization	Chen et al., 2014
c.1376G>A	p.Arg459Gln	Homodimerization	Tian et al., 2019



c.1521_1524delTTGT	p.Cys508Argfs*109	Homodimerization	Johnson et al., 2002 Mhanni et al., 2020
c.1549_1574dup	p.Ile525Metfs*102	Homodimerization	Du et al., 2020
c.1589G>A	p.Gly530Asp	Homodimerization	Kisker et al., 1997

## Figures

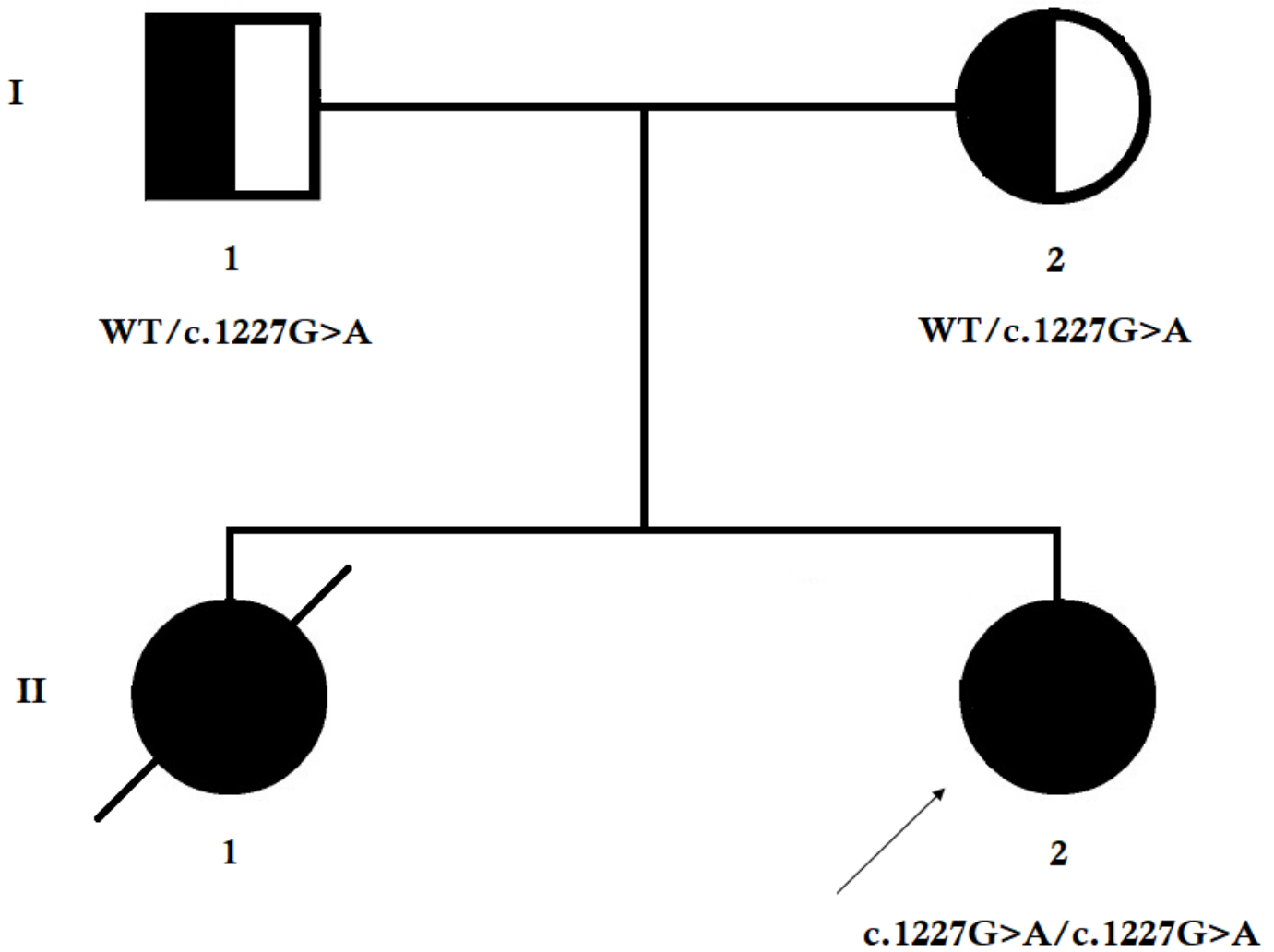


**Figure 1**

Pedigree of the Chinese family with ISOD. Squares and circles denoted males and females respectively. Individuals labelled with a solidus were deceased. Roman numerals indicate generations. Arrow indicates the proband (II-2).

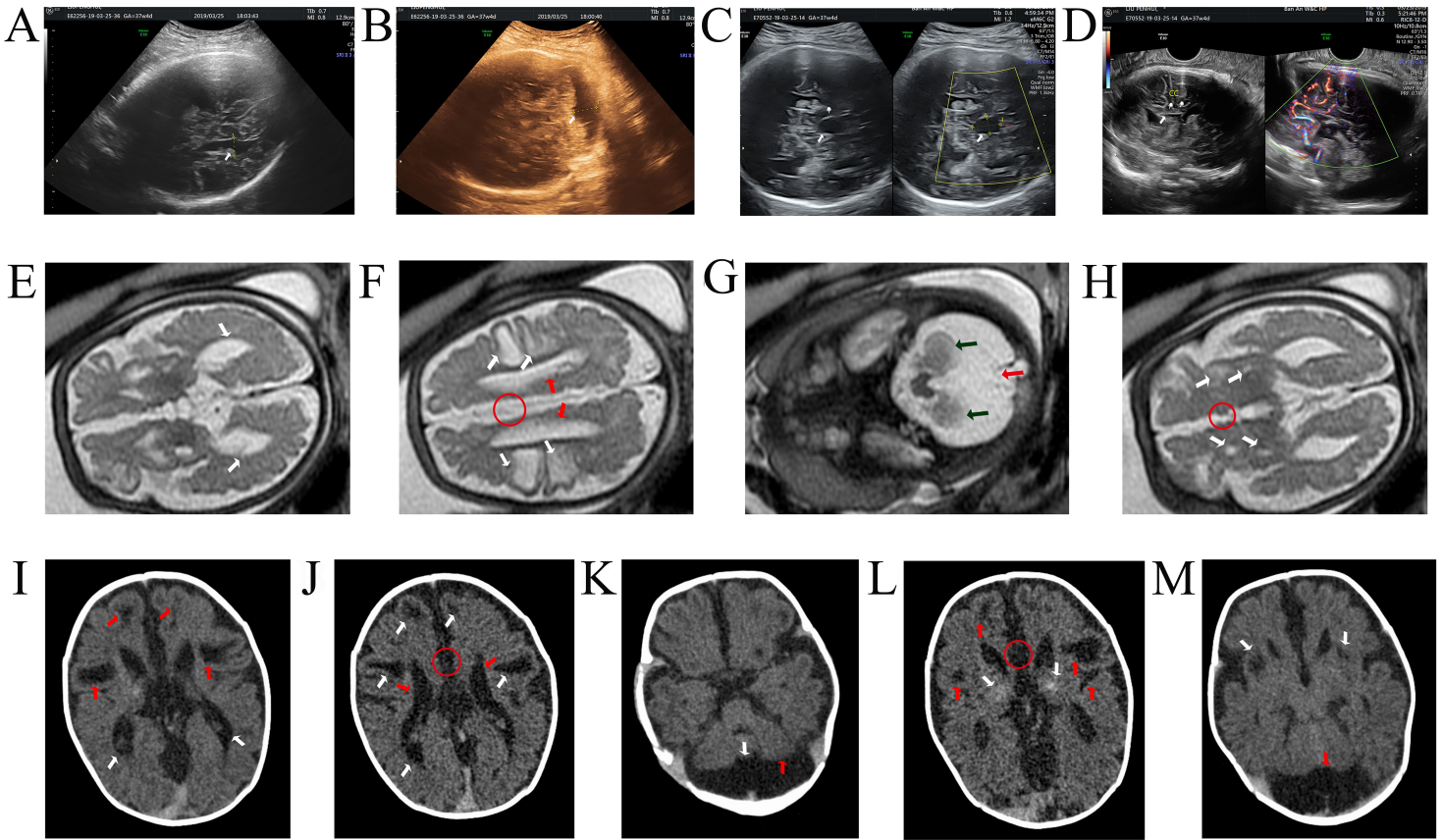


**Figure 2**

A-D. Ultrasonography examination. A. The width of the left lateral ventricle was 1.12 cm (white arrow). B. The depth of cisterna magna was 1.44 cm (white arrow). C. A 1.6\*0.9 cm cystic structure was identified in the midline falx. D. The agenesis of the corpus callosum and the posterior part of the pericallosal artery not showed completely. E-H. Magnetic Resonance Imaging (MRI) examination. E. The axial T2WI images found that the anterior horns of the bilateral ventricle were slightly enlarged (white arrow). The width of them were 11.2mm in left and 10.2 mm in right. F. The axial T2WI images showed several flake-shape foci with T2WI high signal intensities (white arrow) symmetrically demonstrated in the white matter of bilateral frontal and parietal lobes. The longitudinal fissure of the brain was enlarged, and the knee of the corpus callosum was not detected (red circle). The bilateral ventricles were enlarged and parallel with the length of the midline (red arrow). G. The axial T2WI images identified that the cisterna magna was severely enlarged (red arrow) with T2WI high signal intensity. The compressed skull showed in the corresponding part. The bilateral cerebellar hemispheres were small (black arrow). H. The axial T2WI images demonstrated several round-shape foci with T2WI high-signal intensity (white arrow) in the white matter of the right frontal lobe, left basal ganglia and bilateral insular lobes. The longitudinal fissure of the brain was enlarged, and the knee of the corpus callosum was not detected (red circle). I-M. Computed tomography (CT) examination. I. The posterior portions of bilateral ventricle were identified with slight ventriculomegaly (white arrow). The bilateral frontal lobe showed the patchy low-density shadow (red arrow). J. Several patchy low densities (white arrows) symmetrically demonstrated in the white matter of bilateral frontal and parietal lobes. The longitudinal fissure of the brain was enlarged, and the knee of the corpus callosum was not detected (red circle). The distance between the bilateral ventricles was increased and parallel with the length of the midline (red arrow). K. The cisterna magna was significantly enlarged (white arrow), and the bilateral cerebellar hemispheres were small (red arrow). L. The bilateral basal ganglia showed slightly high density (white arrow). Several patchy low-density shadows were identified under the bilateral frontal and parietal cortex (red arrow); the longitudinal fissure was enlarged (red circle). M. The bilateral insular lobes showed patchy and low-density lesion (white arrow). The cisterna magna was severely enlarged (red arrow).

*SUOX*; NM\_000456; c.1227G>A; p.Trp409\*

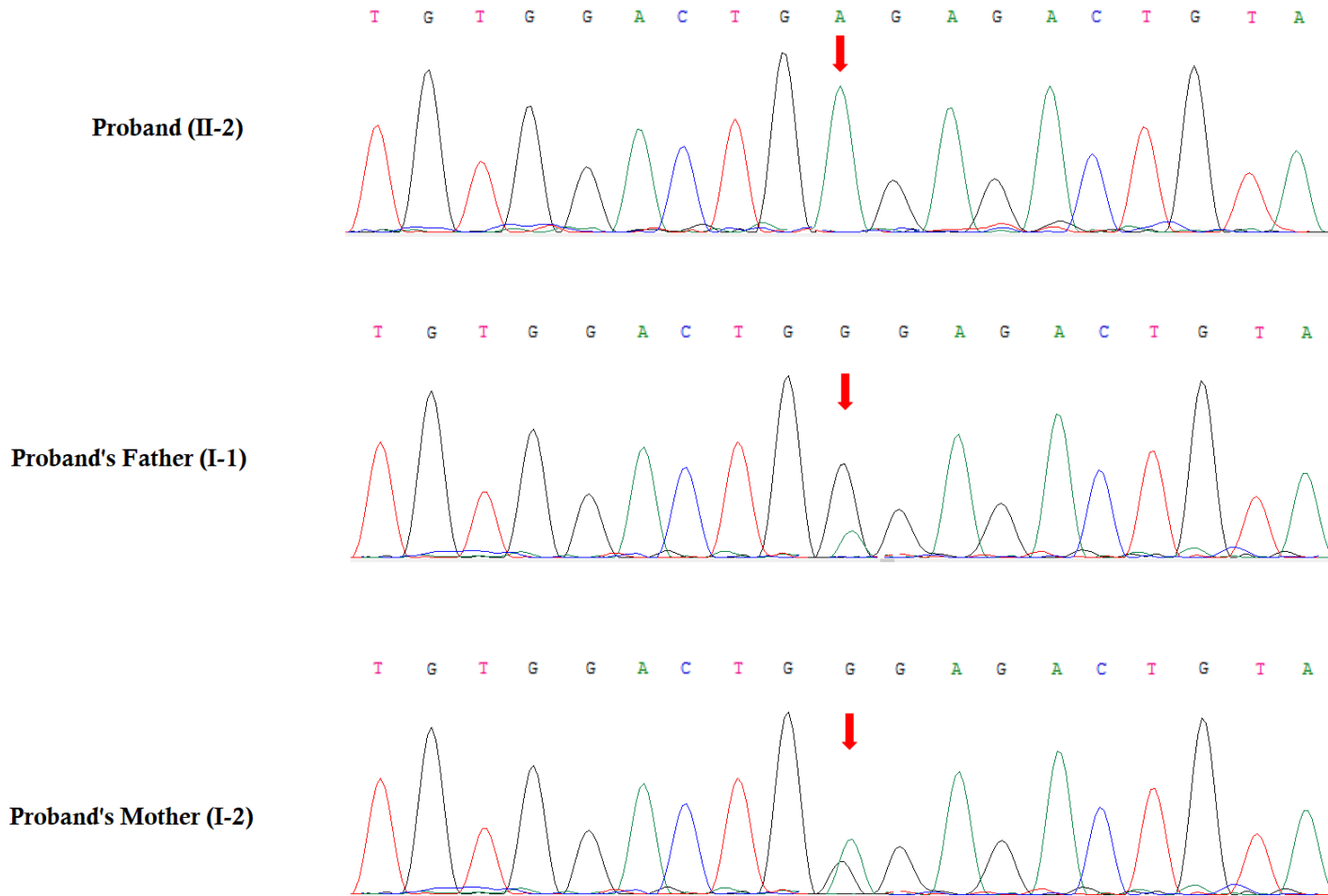


Figure 3

Partial DNA sequences in the *SUOX* gene by Sanger sequencing of the family. The reference sequence NM\_000456 of *SUOX* gene was used.

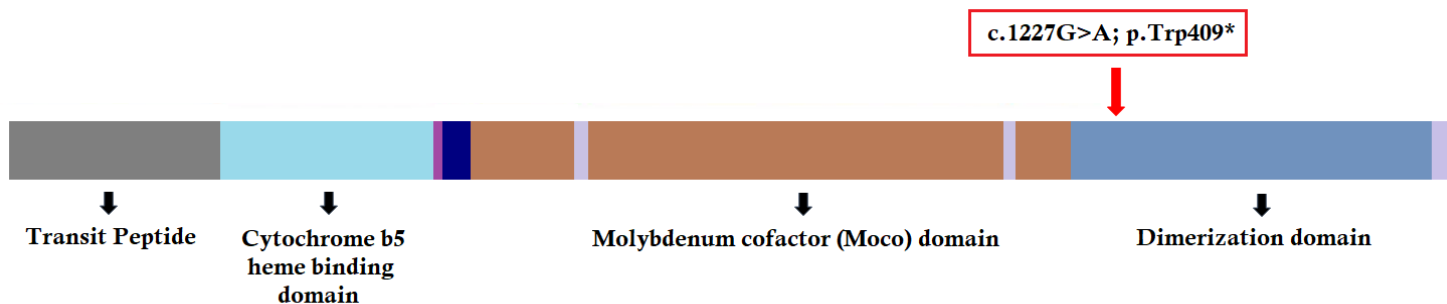


Figure 4

Schematic presentation of Sulfite oxidase.